

# Damage detection and quantification in deck type arch bridges using vibration based methods and artificial neural networks

N. Jayasundara<sup>1</sup>, D.P. Thambiratnam<sup>2</sup>, T.H.T. Chan<sup>2</sup>, A. Nguyen<sup>3</sup>

<sup>1</sup> Queensland University of Technology – Australia, Email: [walpola.jayasundara@hdr.qut.edu.au](mailto:walpola.jayasundara@hdr.qut.edu.au) <sup>2</sup> Queensland University of Technology – Australia, <sup>3</sup>University of Southern Queensland - Australia

## **Abstract:**

Vibration based methods can be used to detect damage in a structure as its vibration characteristics change with physical changes in the structure. Extensive research has been carried out on the use of such methods to detect damage in a number of simple and some complex structures. Arch bridge is a popular type of bridge with rather complex vibration characteristics which pose a challenge for using existing vibration based methods to detect damage in them. Further, its complex form of damage detection, even with modified vibration based methods makes the quantification process harder and challenging. This paper develops and applies a vibration based method especially suited for arch bridges to detect, locate and quantify damages in the structural components. In the proposed method, modified forms of the modal flexibility (MMF) and modal strain energy (MMSE) based damage indices coupled with the Artificial Neural Network (ANN) technology is used to provide an overall damage assessment. The procedure to detect and locate damage was experimentally validated and applied to a full scale long span arch bridge under a range of damage scenarios. Damage indices obtained from noise polluted vibration data are then used as input data for training and validation of the neural networks. Two neural networks were trained separately using MMF and MMSE damage indices and a network fusion approach is used to obtain unambiguous and accurate results for detecting, locating and quantifying damages. The trained neural network system was then successfully applied to identify unknown damages using only vibration data of damaged structural elements of arch bridges. The findings of this paper will contribute towards the safe and efficient operation of arch type bridges.

## **Keywords**

Bridge failures; Arch bridges; Vibration based damage detection (VBDD); Artificial neural networks (ANN); Non-destructive testing

## **1. Introduction**

It is evitable for civil structures to gradually accumulate damage due to various causes such as environmental changes, material aging, variation of load characteristics, inadequate

maintenance etc. These structures need to be monitored, especially those that are aging, so that any damage is detected at the onset and appropriate retrofitting carried out to ensure that they are capable of providing safe and reliable service without unexpected failures. With this in mind, research in this area has attracted much attention over the years and there has been considerable research on damage detection in simple and complex structures. **Studies by Rizos et al. [1] explain the crack detection in beams using natural frequency and vibration modes. The use of wavelet transform of the fundamental mode of vibration was demonstrated by Hong et al. [2] in damage detection of beams. Damage identification studies using vibration based methods such as modal strain energy, mode shape based methods or multi criteria approaches have been carried out to obtain precise damage identification results in plate elements by Shih et al. [3] and Cornwell et al. [4]. These methods were also successfully used for detecting and locating damage in truss structures [5-7]. Furthermore, it has been shown that damage detection methods such as the modal flexibility method, modal strain energy method and derivatives of mode shape data can also be advantageously used to predict damage in complex structures such as offshore platforms by Wang et al. [8], a range of bridge structures such as truss bridges by Shih et al. [9] and Wang et al. [10], slab on girder bridges by Shih et al. [11] and suspension bridges by Wickramasinghe et al. [12] and also in full scale buildings by Wang et al. [13].**

Vibration-based damage detection (VBDD) techniques are global methods [14] which examine the changes in vibration properties between the healthy and damaged states of the structure to evaluate the damage. Natural frequency has been the parameter used in one of the common approaches as it can be easily measured from just a few accessible points [15]. But in many cases, they are insensitive to some structural damages [16]. The modal flexibility (MF) method, first proposed by Pandey and Biswas [17] has been used in many damage detection studies due to its accuracy, ease of application and convenient computation [3, 18]. This method has been successfully applied in a wide range of Structural Health Monitoring (SHM) and damage detection cases [17, 19, 20].

Modal strain energy (MSE) method is found to be another widely applied VBDD method firstly proposed by Stubbs et al. [21]. This has been then used by many researchers utilizing different measured data for different types of structures [6, 7]. However, the application of these methods for damage detection in arch bridges is not prevalent in the literature. Arch bridges exhibit their own particular vibration characteristics which are rather complex and involve the deck, arch rib and the struts (columns). Traditional VBDD methods such as the original forms of MF and MSE methods have been found to perform poorly in detecting damage in arch bridge

components [22]. A dual-criteria approach which simultaneously uses damage indices (DIs) based on modified forms of the MF and MSE methods was therefore developed to successfully detect and locate in arch bridges as presented in [22]. This method is further developed in this paper by combining with artificial neural network (ANN) technology and applied to detect, locate and quantify damage in arch bridge structures.

ANN is a machine learning method which is capable of pattern recognition, classification, self-organizing and nonlinear modelling [23-25]. A well trained neural network is capable of extracting and obtaining precise and reliable information from imprecise, unreliable, inconsistent, uncertain, and noise-polluted data [26] and train itself to provide accurate outputs to given unknown inputs.

The application of DIs based on vibration data with ANN to quantify damage is limited in the literature and hardly applied to full scale structures. There are some studies on detecting and quantifying damage in beams [27], frames [28], multi storey building models [29] and bridge models [30-33] using both vibration data and ANN. Most of these studies utilized vibration data such as frequency, mode shape based parameters as inputs to train the neural networks. Some studies applied the traditional modal flexibility [34] or modal strain energy [32] damage indices to create the ANN input for damage detection. But the conclusions highlighted some false alarms and restricted the proposed methods in those studies to limited damage cases [32]. Further, these approaches are unique to the structure in which the original network was derived and the methods may not be applicable to complex full scale structures such as arch bridges. This problem is addressed in this research by modifying the traditional DIs and developing the ANN architecture accordingly to obtain accurate damage assessment results. The feasibility of the proposed method is demonstrated through its application to a range of damage detection (DD) scenarios.

## **2. Modified VBDD methods to detect damage**

Arch bridges exhibit 3D and rather complex vibration characteristics. The initial global modes of vibration of the whole arch bridge are governed by the mode shapes of the arch rib with dominant contributions in the lateral and vertical directions, in which the maximum mass participations occur.

Therefore, instead of using the resultant mode shapes as in the traditional DIs, decomposed mode shapes using the lateral and vertical components are used to create modified DIs to be

used in this study. To facilitate the use of these component-specific features, the DIs are modified as follows

## 2.1 Modified MF method

According to Pandey and Biswas [17], the modal flexibility change (MFC) can be expressed in the following form (Equation 1), where  $d$  and  $h$  denote the damage and healthy conditions, respectively

$$MFC = [F]_d - [F]_h = \left[ \sum_{i=1}^n \frac{1}{\omega_i^2} \phi_i \phi_i^T \right]_d - \left[ \sum_{i=1}^n \frac{1}{\omega_i^2} \phi_i \phi_i^T \right]_h \quad (1)$$

Modal Flexibility Damage Index (MFDI) is obtained by dividing MFC value of a particular location by MF value of that same location in the healthy state. Therefore, the normalized DI at location  $j$  at  $i^{\text{th}}$  mode can be written in the following form (Equation 2).

$$MFDI_{ij} = \frac{\left[ \sum_{i=1}^m \frac{1}{\omega_i^2} \phi_i \phi_i^T \right]_D - \left[ \sum_{i=1}^m \frac{1}{\omega_i^2} \phi_i \phi_i^T \right]_H}{\left[ \sum_{i=1}^m \frac{1}{\omega_i^2} \phi_i \phi_i^T \right]_H} \quad (2)$$

The modified modal flexibility DI can then be derived by decomposing the mode shapes into lateral and vertical components and hence creating two indices component specific DIs denoted as  $MFDI_L$  and  $MFDI_V$  as given in Equations (3) and (4). Subscripts L and V denote the lateral and vertical components.

$$MFDI_{ijV} = \frac{\left[ \sum_{i=1}^m \frac{1}{\omega_i^2} \phi_i \phi_i^T \right]_{DV} - \left[ \sum_{i=1}^m \frac{1}{\omega_i^2} \phi_i \phi_i^T \right]_{HV}}{\left[ \sum_{i=1}^m \frac{1}{\omega_i^2} \phi_i \phi_i^T \right]_{HV}} \quad (3)$$

$$MFDI_{ijL} = \frac{\left[ \sum_{i=1}^m \frac{1}{\omega_i^2} \phi_i \phi_i^T \right]_{DL} - \left[ \sum_{i=1}^m \frac{1}{\omega_i^2} \phi_i \phi_i^T \right]_{HL}}{\left[ \sum_{i=1}^m \frac{1}{\omega_i^2} \phi_i \phi_i^T \right]_{HL}} \quad (4)$$

## 2.2 Modified MSE method

According to Stubbs et al. [35] MSE damage index  $\beta_{ij}$  for  $j^{\text{th}}$  member at  $i^{\text{th}}$  mode can be expressed as Equation (5) below where  $k_j$  is the bending stiffness of the beam and  $\phi_i(x)$  is the mode shape of  $i^{\text{th}}$  modal vector. All the modal parameters associated with damaged structure are denoted by asterisks

$$\beta_{ij} = \frac{k_j}{k_j^*} = \frac{\left( \int_j [\phi_i^{*''}(x)]^2 dx + \int_0^L [\phi_i^{*''}(x)]^2 dx \right) \int_0^L [\phi_i''(x)]^2 dx}{\left( \int_j [\phi_i''(x)]^2 dx + \int_0^L [\phi_i''(x)]^2 dx \right) \int_0^L [\phi_i^{*''}(x)]^2 dx} \quad (5)$$

The above equation can also be given in the following form (Equation 6).

$$\beta_{ij} = \frac{k_j}{k_j^*} = \frac{[(\phi_i^{*''})^2 + \sum (\phi_i^{*''})^2][\sum (\phi_i'')^2]}{[(\phi_i'')^2 + \sum (\phi_i'')^2][\sum (\phi_i^{*''})^2]} \quad (6)$$

The MSE-based method can be similarly modified to give the two decomposed damage indices  $\beta_{ijV}$  and  $\beta_{ijL}$ ; which denotes the vertical and lateral component specific DIs using the lateral and vertical components of mode shapes respectively.

For both methods, a single indicator is generated by taking several global modes into account as follows.

$$MFC = [F]_d - [F]_h = \left[ \sum_{i=1}^n \frac{1}{\omega_i^2} \phi_i \phi_i^T \right]_d - \left[ \sum_{i=1}^n \frac{1}{\omega_i^2} \phi_i \phi_i^T \right]_h \quad (7)$$

In the above equation, NM refers to the number of modes, and  $Num_{ji}$  and  $Denom_{ji}$  are the numerator and denominator of anyone the Equations (3), (4), (5) or (6), depending on the particular DI.

As observed previously [22] one of the component specific DI, based on either MSE or MF method, can perform better than the other, depending on the location of the damage, The numerical value of this component DI will be higher compared to the other component DI. Therefore to obtain the best possible results it is necessary to select (and use) the component specific DI which performs better than its counterpart, for both MF and MSE based DIs. Towards this end, the above modal flexibility and modal strain energy methods can be further **modified as shown in Equations 8 and 9 respectively.**

For the MSE case, the better performing DI is selected by comparing the results of  $\beta_{jV}$  and  $\beta_{jH}$ . The same is done with the 2 component specific MFDIs. That is for damage detection at any location the prominent  $\beta_j$  and  $DI$  are obtained by selecting the larger of the two component specific DIs.

$$\beta_j = [\max (|\beta_{jV}| , |\beta_{jH}| ) ] \quad (8)$$

$$DI = [\max (|DI_V| , |DI_H| ) ] \quad (9)$$

The selected  $\beta_j$  and  $DI$  are then normalized as shown in Equation (10) below, in which  $\bar{\beta}$  and  $\bar{DI}$  are the mean values and  $\sigma_\beta$  and  $\sigma_{DI}$  are standard deviations of  $\beta_j$  and  $DI$  respectively.

$$Z_j = \frac{\beta_j - \bar{\beta}}{\sigma_\beta} \text{ or } Z_j = \frac{DI - \bar{DI}}{\sigma_{DI}} \quad (10)$$

This method was experimentally validated and details are presented in [22], while a brief description of the validation is presented below for completeness of the present paper.

Experimental validation of the developed method was carried out using the results from the experimental testing of the arch bridge model (Figure 01a). The Bridge model was tested for both intact and damage cases (inducing a cut at the base of the 3<sup>rd</sup> vertical column) (Figure 01c). Free vibration testing was performed on the bridge model (Figure 01b) to obtain the vibration parameters of mode shapes and natural frequencies to validate the proposed damage detection method. Four component specific damage indices were calculated using the experimental data and then the better performing DIs were selected using the procedure outlined through Equations (8), (9) and (10). These preferred DIs are then used to obtain the damage detection results and thereby verify the proposed method experimentally.

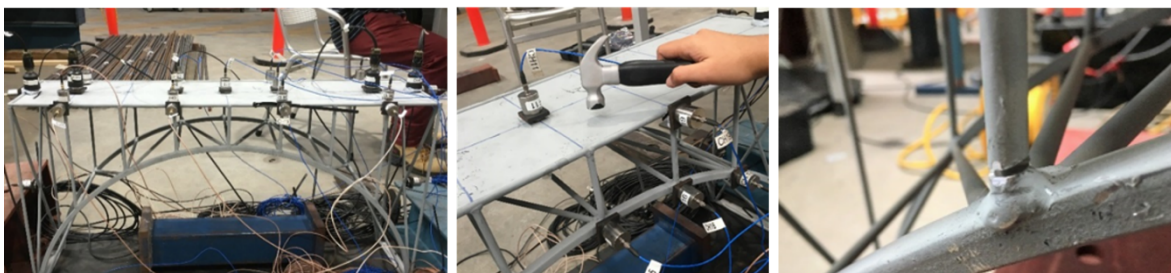
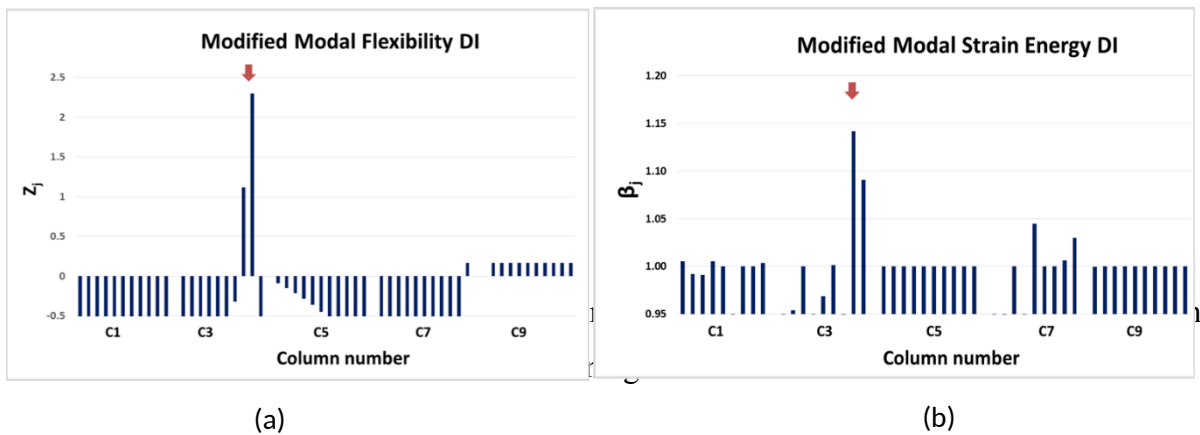


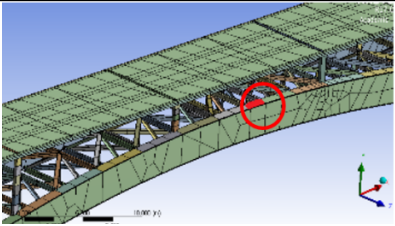
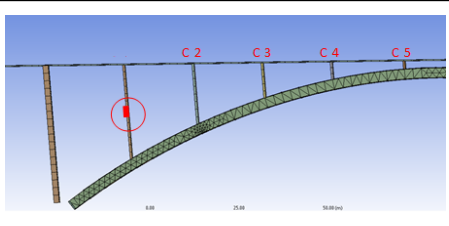
Figure 01: (a) Bridge model with accelerometer arrangement and (b) dynamic test on the bridge (c) damage on the vertical column



It is evident that the damage at 3rd vertical column of the bridge is correctly detected through the method proposed by the peaks of both modified damage indices which clearly indicate the location of damage (Figure 02).

To illustrate the applicability of the proposed damage detection technique to a full scale long span arch bridge, a complete finite element model of 200m long Cold Spring Canyon Bridge was developed and validated [22]. Then to evaluate the performance of above method, 2 damage cases involving damage in the rib and vertical column of this arch bridge were tested and presented below. The damage was introduced as 10% stiffness reduction at a small part on the rib or column.

Table 1: Damage Scenarios of the Cold Canyon arch bridge

Damage Scenario		
	Rib Damage Case	Vertical column damage Case

Damaged Element	Damage at crown	Damage at mid of the long column
Stiffness Reduction	10%	10%

- Rib Damage Case: Damage at mid span of the arch rib

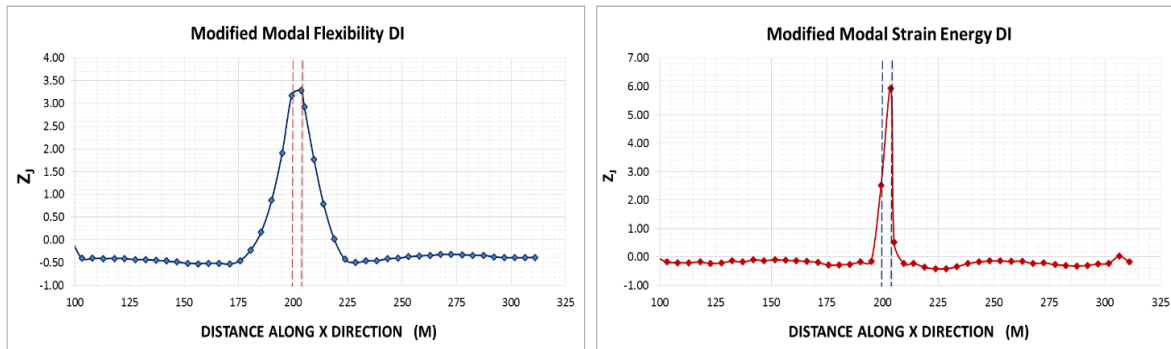


Figure 03: Plots of Modified MF and Modified MSE DIs for rib damage case

- Vertical Column Damage Case: Damage at mid span of the first column C1.

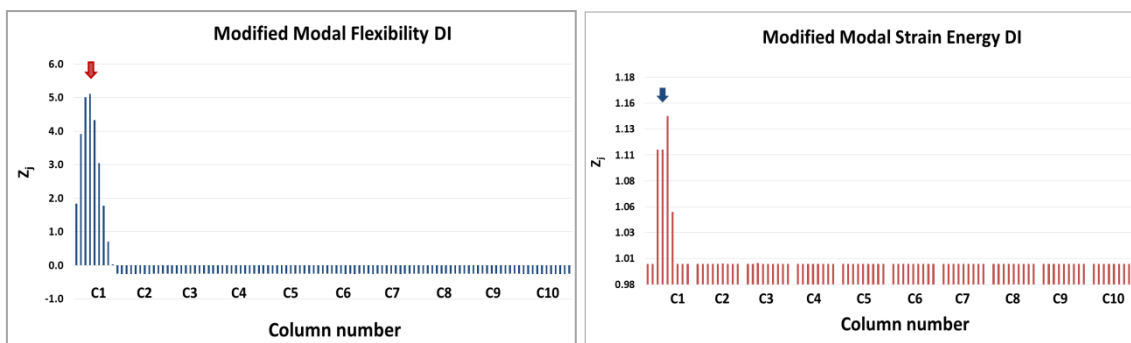


Figure 04: Plots of MMF and MMSE DI for damage at the middle of long column C1

Figure 03 and Figure 04 present the modified Modal Strain Energy and Modified Modal Flexibility DI plots of the two damage cases presented in Table 1. All four graphs clearly indicate sharp peaks at the damage locations in the arch rib and the column. These results confirm that the proposed dual criteria approach gives correct and unambiguous results. This method is hence further developed by incorporating ANN to provide complete damage assessment (to detect, locate and quantify) in the structural components of arch bridges.



### 3. Damage quantification in arch rib and vertical columns using modified versions of MF and MSE

Quantifying damage is generally very challenging compared detecting and locating damage. There are a few references available in the literature on damage quantification for beams [36, 37] and trusses [38]. But these numerical methods are not generic and are specific for a particular structure in which it was initially tested. Therefore these methods may not be applicable to quantify damage in complex structures or their components. With a view of addressing this issue, this study analysed the performance of the modified DIs for assessing damage at different locations and at different intensities along the arch rib and vertical columns to understand their capability to treat arch ribs and columns of arch bridges. Figure 05 illustrates the variation of MMSE DI curves for 22 damage cases along the arch rib of Cold Canyon bridge for 10%, 15%, and 20% damage severities. It is evident that higher the damage severity, higher the peaks of the DI. Most importantly, these graphs clearly exhibit that the peaks of the DI curves for the same damage intensity vary depending on the damage location in the rib and on the boundary conditions of the bridge. A similar pattern emerged when the MMF DI was investigated.

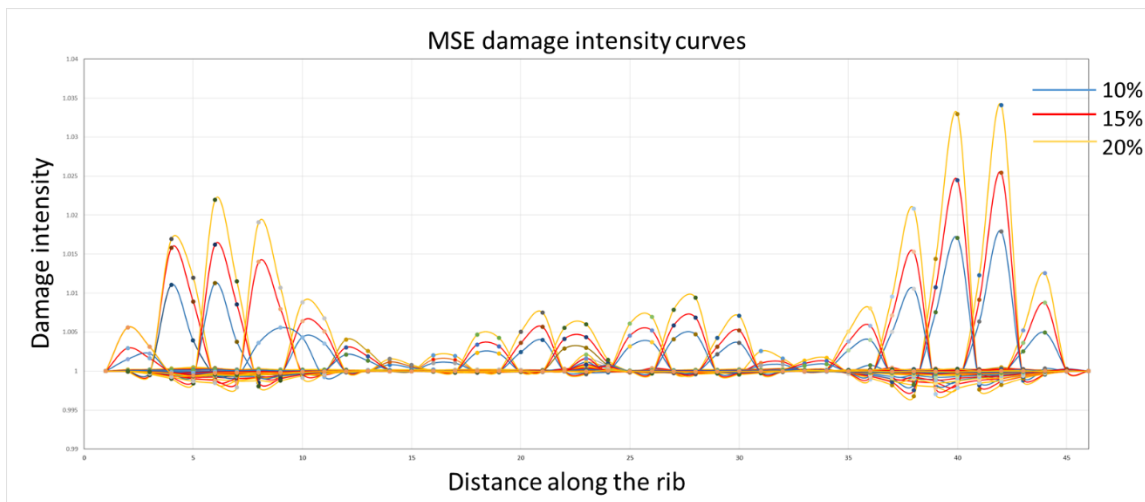
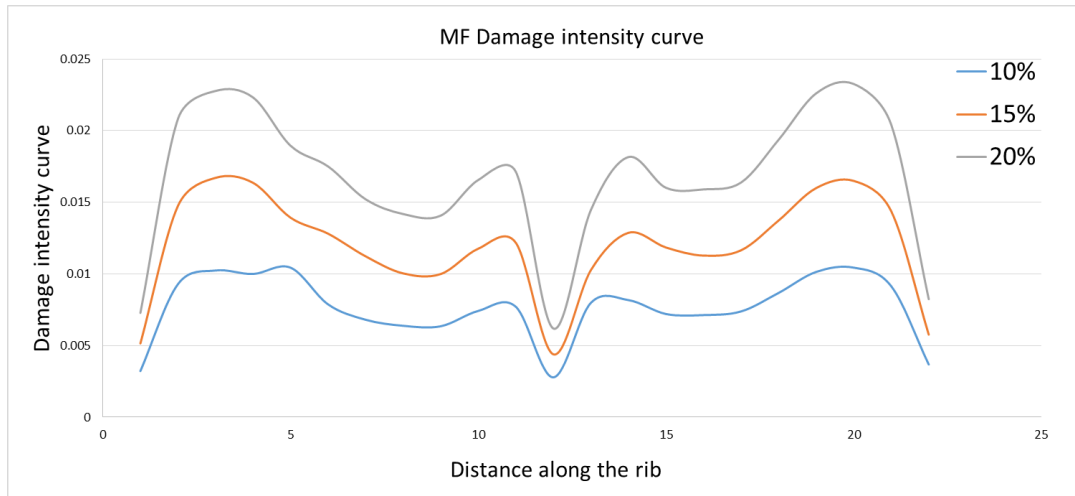


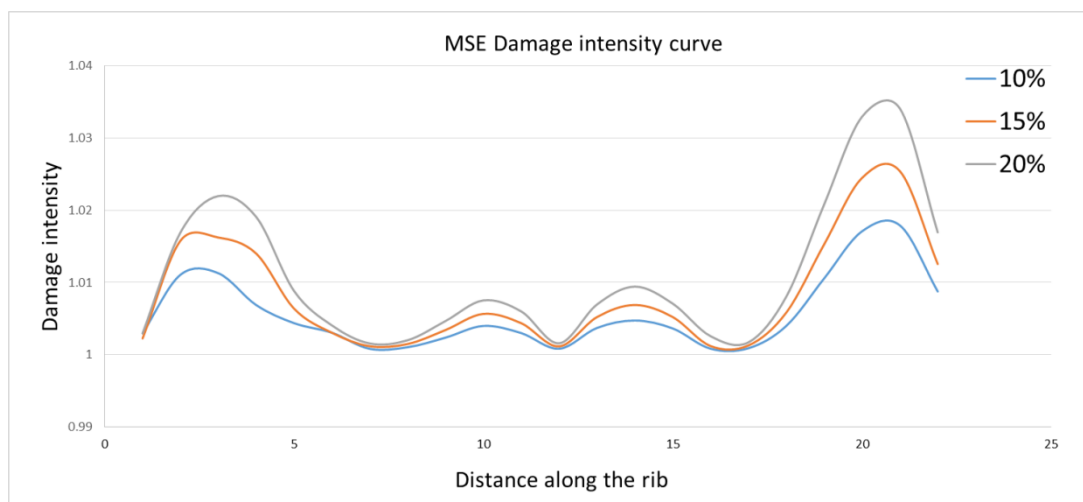
Figure 05: Plots of MSE damage intensity curves for 10%, 15%, and 20% damage

Using the information from the above investigations, Figures 06 (a) and 06 (b) illustrate the variations of peaks of MMF DI and MMSE DI curves respectively for 10%, 15% and 20% damage intensities for 22 locations along the rib. These two plots confirm that the damage intensity curves seem to exhibit certain patterns: (i) There are higher peaks near the edges for the same damage intensity and (ii) Peak values increase with increasing damage intensity.

These patterns can cause problems, when the damage location and intensity are not known (as in the inverse problem).



(a)



(b)

Figure 06: Plots of (a) MMF (b) MMSE damage intensity peak curves for 10%, 15% and 20% damage

Variations of MMF DIs for damage along the long and short vertical columns was then studied. Figure 07 illustrates 3 damages (at different locations) in one of the longer columns (column 01) and Figure 08 illustrates the plots of MMF DIs for 3 damage cases in a short column (column 04). The damage locations on the columns are denoted by red cross marks on the

relevant columns. It is evident that the DIs plots are clear without false alarms for long columns but they display some false alarms and disturbances for short columns.

Similar observations were made when the MMSE DI was tested. There is hence a need for a dependable and a precise method to understand the behaviour of the DI curves along the arch rib and across the columns (or vertical struts) under different damage severities. With this in mind, an artificial neural network was trained to learn the behaviour of DI curves along the rib and vertical columns and thereby retrieve the damage location and severity of unknown damage when the vibration properties (mode shapes and frequencies) are available.

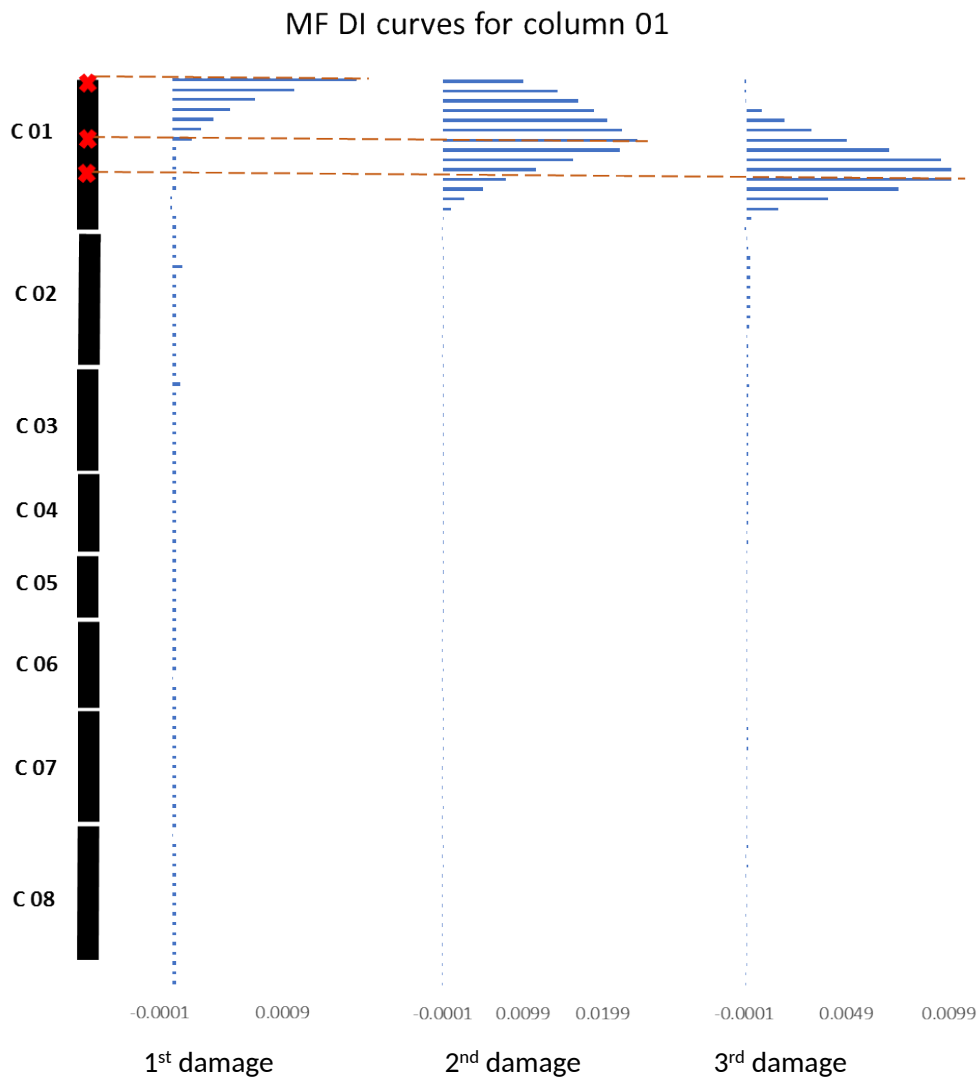


Figure 07: Plots of MMF damage index curves for 3 damage cases on long column (Column 01)

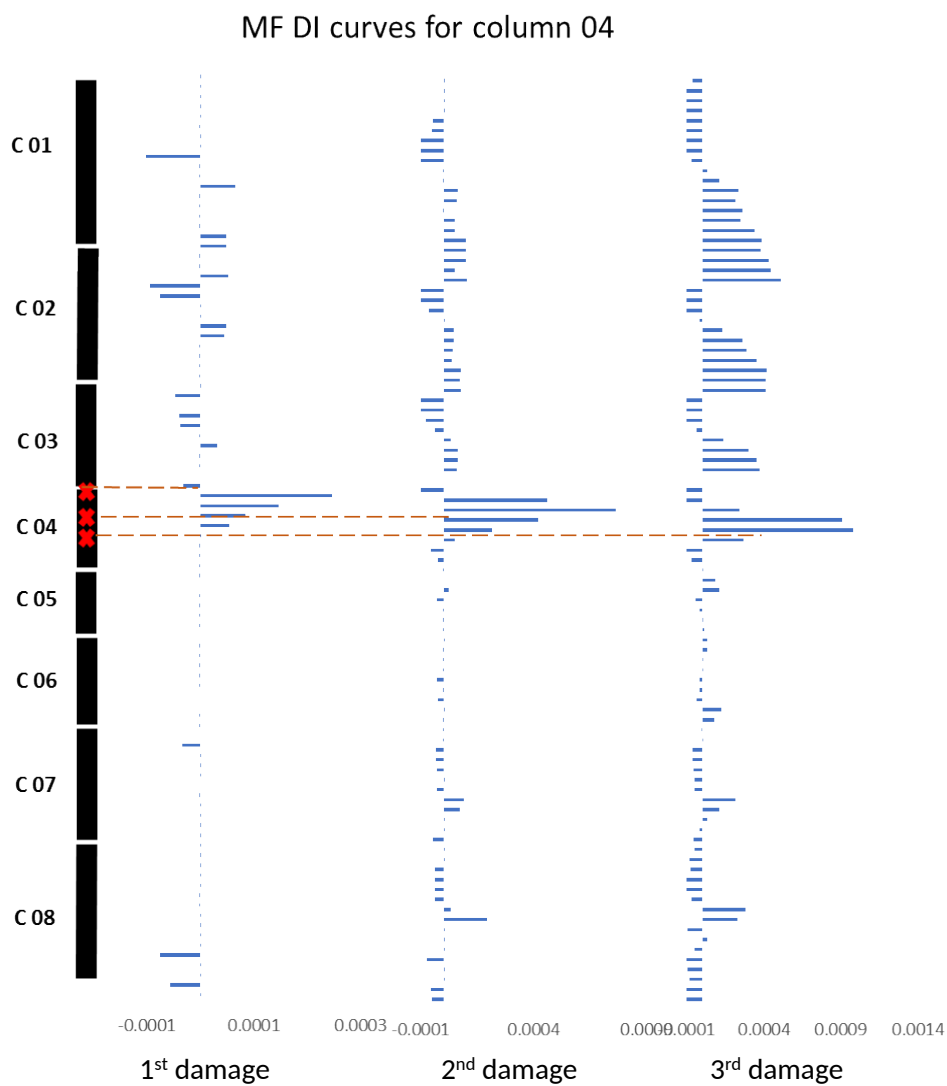


Figure 08: Plots of MMF damage index curves for 3 damage cases on short column (column 04)

#### 4. Artificial Neural Network

The artificial neural network (ANN) is an advanced machine learning technique that operates in a manner analogous to that of biological nerve systems. It is capable of learning and developing its own algorithm using given input and output data. ANN consists of weighted interconnected neurons which connect the input, hidden and output layers. The neuron weights are modifiable and are offset by a constant and learning is achieved by adjusting the connections (weights) in the network to minimize a specific performance index (e.g., the mean square error at its output). The layers are linked by transfer functions. Multi-layer feed forward neural network with back-propagation algorithm is the most common type of network used in most civil engineering applications. A schematic model of a four-layer neural network is shown in Figure 09. When the input samples are fed to the network, the outputs are compared with the targets using generalized learning algorithms while minimizing the error function. Once the mean square error becomes a minimum, the training stops. The trained network is then used to test a set of new input parameters.

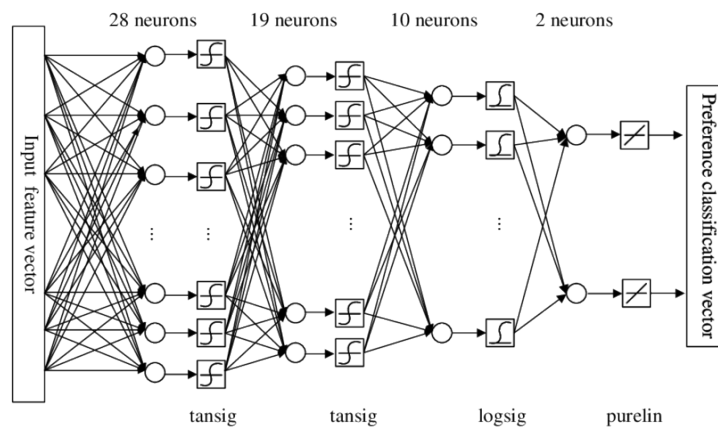


Figure 09: A schematic model of a four-layer neural network

## 5. Methodology

As mentioned earlier the aim of this paper is to develop and present a vibration-based method to locate and quantify damage in arch bridge structural components using DIs based on modified versions of (traditional) MSE and MF methods and ANN. ANNs are utilized to map pattern changes of DIs to damage characteristics.

Validated full scale numerical arch bridge finite element (FE) model is used as the baseline structure to build the ANN. The arch rib and vertical columns being the subjects of interest to develop the ANN. Firstly the vibration data (i.e mode shapes and frequencies) are obtained for

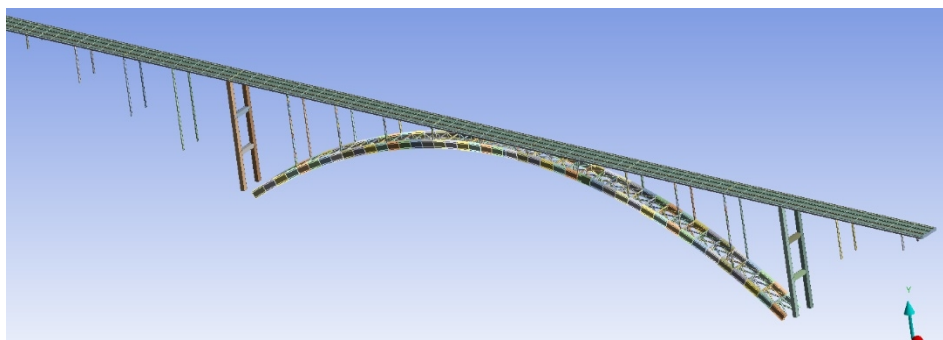
intact and damaged structure for a range of damage scenarios. To simulate field-testing conditions, white Gaussian noise is added to the numerical data. The MMF and MMSE DIs are calculated separately using the equations presented earlier. Then two neural networks were trained by inserting DIs of known damages as inputs and damage location and severity as outputs. Finally, two individual networks are fused together and an overall damage prediction model is obtained.

### 5.1 Numerical model of full scale arch bridge

To illustrate the applicability of the proposed damage detection technique to a full-scale long-span arch bridge, a complete FE model of 213m Cold Spring Canyon Bridge is developed using ANSYS FE modelling software (Figure 10(b)). Cold Spring Canyon Bridge is a long-span, deck type steel arch bridge with a span of 213 m and a rise of 36.27 m. The main ribs are restrained except for the rotational degrees-of-freedom about the transverse axis at the abutments, thus creating a two hinged arched mechanism (Figure 10(a)). The bridge was modelled as a 3D FE model with several parts (deck, arch ribs, cross bracings, columns etc.) which were ultimately connected via relevant connectivity (joint feature) in the Mechanical module. The model and applicability of the modified damage indices have been validated and presented in [22].



(a)



(b)

Figure 10: (a) Real cold canyon bridge (b) Finite element model of the bridge

## 5.2 Data extraction and pre-processing

Input data for the neural network should contain compressed information on the damage features, should be highly sensitive to damage and should be capable of expressing the identical pattern of damage variations at different locations. Since the above sections explained the versatility of the proposed DIs to predict the exact damage location, MMSE DIs and MMF DIs were selected to create input parameters to neural network.

The Bridge model was tested for a series of damaged and non-damaged cases and the data was converted to DIs to create input data to neural network. Rib damage was inflicted at 45 different locations along the arch rib creating 45 damage location cases. Column damages were inflicted at 15 different locations per column and for all 10 columns at one side of the bridge. For both rib and column damage cases 5 damage intensity levels were created by inducing different stiffness reductions. This was done by reducing Young's modulus by 5%, 10%, 15%, 20% and 25%. All the extracted data were polluted with 1%, 2%, and 5% white Gaussian noise to simulate environmental influence on data and another single set was used without noise pollution. Noise contaminated mode shapes prepared using Equation (11) presented in [6] was used to create the noise polluted data for neural networks. This will create 900 rib DI curves and 3750 column DI curves for each method to be used as input data for ANNs.

$$\overline{\phi}_{xi} = \phi_{xi}(1 + \gamma_x^\phi \rho_x^\phi |\phi_{max,i}|) \quad (11)$$

The terms  $\overline{\phi}_{xi}$  and  $\phi_{xi}$  are mode shape components of the  $i^{\text{th}}$  mode of vibration at location  $x$  with and without noise respectively.  $\rho_x^\phi$  denotes the random noise level and  $\gamma_x^\phi$  refers to a random number with mean equal to zero and variance equal to 1 and  $|\phi_{max,i}|$  is the absolute value of the largest component in the  $i^{\text{th}}$  mode shape.

## 5.3 ANN architecture

To identify the damage locations and severities, supervised feed-forward multi-layer neural networks are designed. The DIs are used as input patterns to the networks while the output is the corresponding damage severity and the location. For each element type (Rib and column) two separate networks are designed for MMF and MMSE input data.

The number of input nodes and output nodes of each network are chosen to match with the number of variables in the input and output data sets. The number of hidden layers was decided

through a trial and error process to obtain minimum mean square error. Once the network configuration is decided, few trials need to be done even with the finalised network configuration, to obtain the best convergence and minimum error. The reason behind this practice is that each training on neural network assigns different weights on neurones and initial conditions, which will ultimately result in different trained networks with different mean square errors. Following sections describe the selected network configurations to obtain the best outcome.

### 5.3.1 Rib neural network

Each rib neural network consists of an input layer of 45 nodes, representing the number of the data points on the rib. Three hidden layers of 45, 15, and 5 nodes as well as 5 node output layer is selected to estimate the location or the severity of the damage. The design and operation of all neural networks were performed with Matlab.

The outcome of the trained neural network depends on the effectiveness as well as the number of input data. Higher the number of input data, higher the accuracy of the outcome. As illustrated in Section 6.3, the input data itself follows an intricate pattern along the rib to capture damage severity. Therefore the number of variables the network has to handle is comparatively higher. This will automatically demand more input data, which means a huge amount of damage trials (cases). Since this study uses a limited number of damage cases, a sub-structured network system was introduced so that the number of variables each substructure has to handle is limited and hence the outcome of the final network will be more accurate.

Substructuring was done by splitting the total sample space into 5 segments. This segment division was decided by analysing the input data patterns. After examining the graphs given in Figure 05 and 06 it was evident that all the DI curves follow a certain pattern. Therefore according to that pattern, the total length of the rib was divided into five segments as shown in Figure 11.

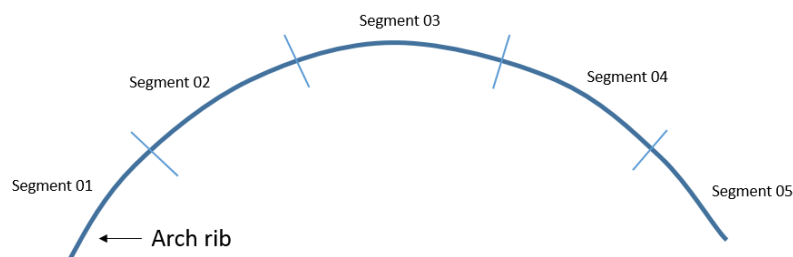


Figure 11: Segments along the length of the arch rib



The neural network was then modified by introducing 5 sub-networks, trained separately on input-output data sets related to each segment. And then all the subcodes were called at the main method (main neural network) so that the program will automatically select the relevant substructure and proceed until the final output.

The sub-networks designed for each substructure has 8 or 10 input nodes; two hidden layers and output node predicting the damage location or severity. Hyperbolic tangent sigmoid functions were the transfer function for all networks. Training is performed using the back-propagation conjugate gradient descent algorithm. The input data is initially divided into three sets; training, validation, and testing. Total sample space is divided into the above 3 sets as 70% (training), 15% (validation) and 15% (testing). The network is designed in a way that while it is training with the training samples, the performance is supervised by the validation set to avoid overfitting. The network training stops when the error of the validation set increases while the error of the training set still decreases, which is the point when the generalisation ability of the network is lost and overfitting occurs. The design and operation of all neural networks are performed with Matlab. Once the network is trained, it is used to detect the damage location and severity of unknown damage cases. When the calculated DI value of unknown damage is fed into the network, it firstly recognises the damage substructure or the area where the damage should be. Then the relevant subnetwork is called upon to predict the exact damage location and its severity, which will retrieve as the output.

### **5.3.2 Column neural network**

A single neural network system can be designed for the columns in the Cold Canyon Bridge as it is symmetrical about its longitudinal axis and hence columns on one side of the bridge are considered for neural network design. As before, the design and operation of all neural networks were performed with Matlab. The main network is trained with around 3750 input data and it is designed to first identify the damaged column. Then it calls the relevant subnetwork, trained for each column separately to further identify the damage location on the column and its severity.

Column network substructuring was done by splitting the total sample space into 10 parts. Thereby each subnetwork represents one column. As discussed in the rib neural network design, all the subcodes were called at the main method so that the program will automatically select the relevant substructure and proceed till the network converges.

As presented earlier, each column was divided into 15, 8 or 5 parts (depending on the height of the column) to induce damage as well as to collect mode shape data at each node location. The neural network (sub network) for one long column therefore comprises an input layer of 15 nodes, representing the number of the data points on a single column; two hidden layers of 15, and an output layer of 15 nodes to estimate the location or the severity of the damage. Training algorithm and the percentage division of input cases are similar to rib networks. Once the networks are trained, they can be used to detect the damage location and severity in unknown damage cases. When the calculated DI value of unknown damage is fed into the network, it firstly recognises the damaged column and then the relevant subnetwork of that column will predict the exact damage location and its severity as the outputs.

## 6. Results and Discussion

Two separate networks as MF network and MSE network were trained (for both rib and columns separately). Then the accuracy of the results obtained by each network is discussed. Further, the advantage of using both methods so as to complement and supplement the required results is explained. Finally, results of both methods are fused into a single system so that only one precise result will be obtained.

### 6.1 MMF Network

The first neural network (main method), which decides the damage substructure has 3 hidden layers, each containing 45, 15 and 5 nodes, respectively for the rib neural network (Figure 12). This is followed by sub-networks which decide the exact damage location and the severity. The network was trained using Levenberg-Marquardt (trainlm) training function. The training process was ceased when the mean square error becomes a minimum. Once the network has been trained with available data, the trained network can be used to obtain damage location and the severity of unknown damage cases. Figure 13 presents the regression plots of trained MMF main method for training, validation and testing sets. Since all coefficients of correlations (R) are more than 0.99, the network is confirmed as appropriately trained.

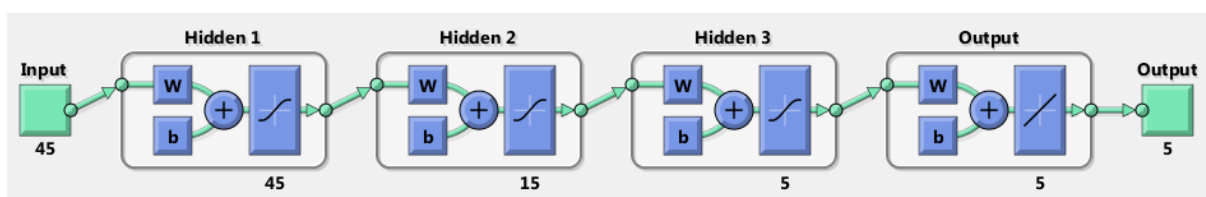


Figure 12: Neural network layout

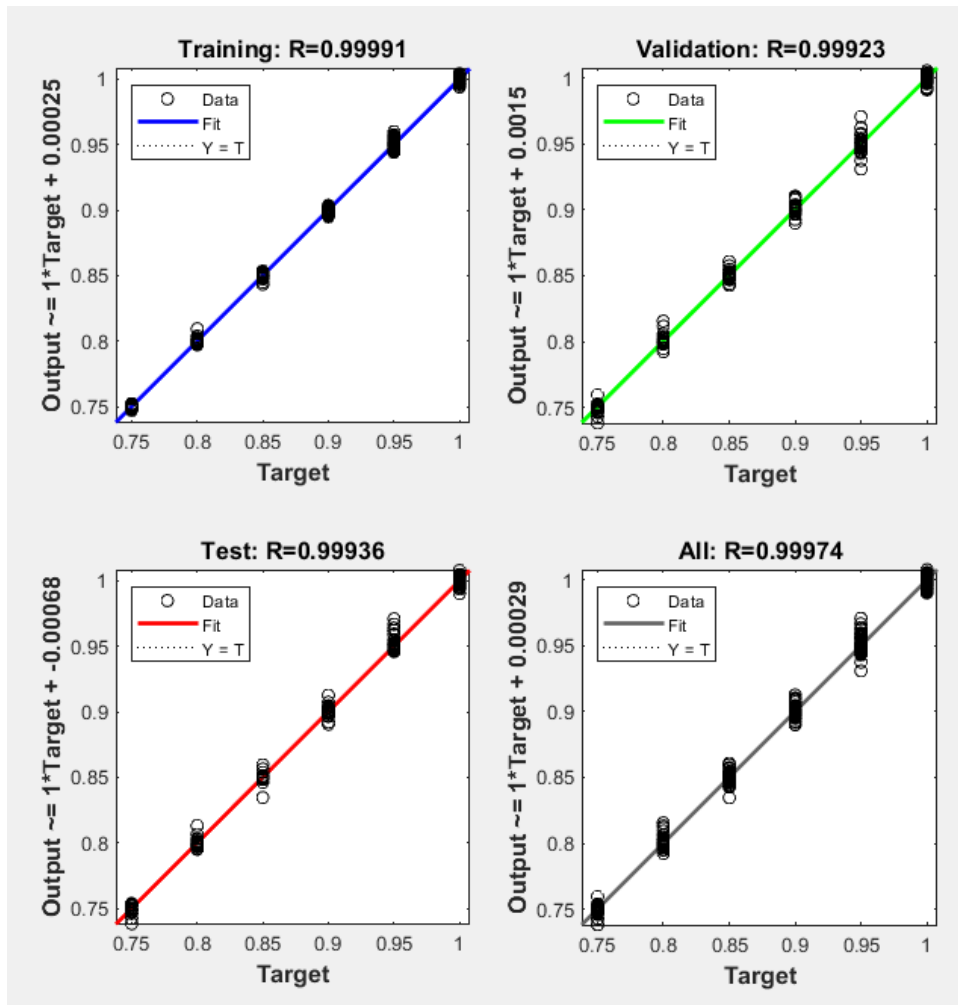


Figure 13: Training, validation and test regression plots of MMF main method

### 6.1.1 Rib damage test

In order to test the ability of the trained network to precisely detect the damage location and the severity of unknown damage, 8 damage cases were created on the FE model and the corresponding vibration properties were extracted. These vibration properties are then used to calculate the modified MF damage indices. These indices are then fed into the trained network and the network prediction was obtained. The following table shows the damage cases tested on a trained network with its expected and received outcomes. It can be seen that the percentage errors of the test cases on MMF neural network are less than 1% and this confirms the compelling performances of MMF neural network to detect, locate and quantify damage. Furthermore, it confirms that the network is capable of interpolating and identify new damage severities which are not experienced during the initial training process

Table 01: MF neural network outcomes for random rib damage cases

Damage case	Absolute damage severity and location		Neural Network outcome		Percentage error in severity prediction
	Severity	Location	Severity	Location	
01	7.5%	X= 190m	<b>7.74%</b>	X= 190 m	-0.26%
02	7.5%	X= 238.5m	<b>7.68%</b>	X= 238 m	-0.19%
03	12%	X= 151.5m	<b>11.85%</b>	X= 152 m	0.17%
04	12%	X= 277.5m	<b>11.52%</b>	X= 277 m	0.88%
05	18%	X=113 m	<b>17.9%</b>	X=113 m	0.12%
06	18%	X=203 m	<b>18.15%</b>	X=203 m	-0.18%
07	22.5%	X= 122 m	<b>22.41%</b>	X= 122 m	0.12%
08	22.5%	X= 233 m	<b>22.61%</b>	X= 233 m	-0.14%

### 6.1.2 Column damage test

In order to test the ability of the trained network to precisely detect the damage location and the severity of an unknown damage, 5 damage cases were created on the vertical columns of the arch bridge FE model and the corresponding vibration properties were extracted. These 5 test cases are completely random and none of these damage severities was used to train, validate or test the neural network at the network training stage. The vibration properties are then used to calculate the MMF based damage indices. These indices are then fed into the trained network and the network predictions were obtained. Each of these test cases was first assigned to the subnetwork of the relevant column and then the subnetwork predicted the precise location and severity. The following table (Table 02) shows the damage cases tested on a trained network with its expected and received outcomes. It can be seen that the percentage errors of the test cases on MMF neural network are less than 1% and this confirms the effective performances of MMF neural network to detect, locate and quantify damage. Furthermore, it confirms that the network is capable of interpolating and identifying new damage severities which are not experienced during the initial training process.

Table 02: MMF neural network outcomes for random column damage cases

Damage case	Absolute damage severity and location		Neural Network outcome		Percentage error in severity prediction
	Severity	Location	Severity	Location	
01	7.5%	Column 1 at Y=27.2m	<b>9.0%</b>	Column 1 at Y=27 m	-1.6%

02	7.5%	Column 2_Y= 40.2m	<b>7.0%</b>	Column 2_Y= 40 m	0.54%
03	12%	Column 3_Y= 46.5m	<b>12.0%</b>	Column 3_Y= 46m	0.0%
04	12%	Column 4_Y= 44.8m	<b>11.5%</b>	Column 4_Y= 44m	0.57%
05	18%	Column 5_Y= 45.2m	<b>16.2%</b>	Column 5_Y= 45m	2.19%

## 6.2 MMSE Network

MMSE main network was trained using Bayesian regularisation (trainbr) training function. There are 2 hidden layers containing 15 and 5 nodes respectively for ribs and 2 hidden layers of 15 nodes for column case. Similar to MMF network, the number of input nodes is 45 and output nodes is 5. Figure 14 presents the network configuration for rib damage. Training was performed to obtain best the fitting algorithm to map the given inputs and output. The training process ceased when the mean square error becomes a minimum. Figure 15 presents the regression plots of trained MMSE main method for training, validation and testing sets. Since all coefficients of correlations (R) are more than 0.99, the network is assumed as trained properly.

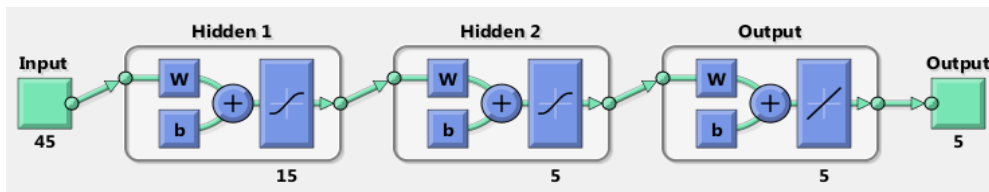


Figure 14: MMSE main method network configuration

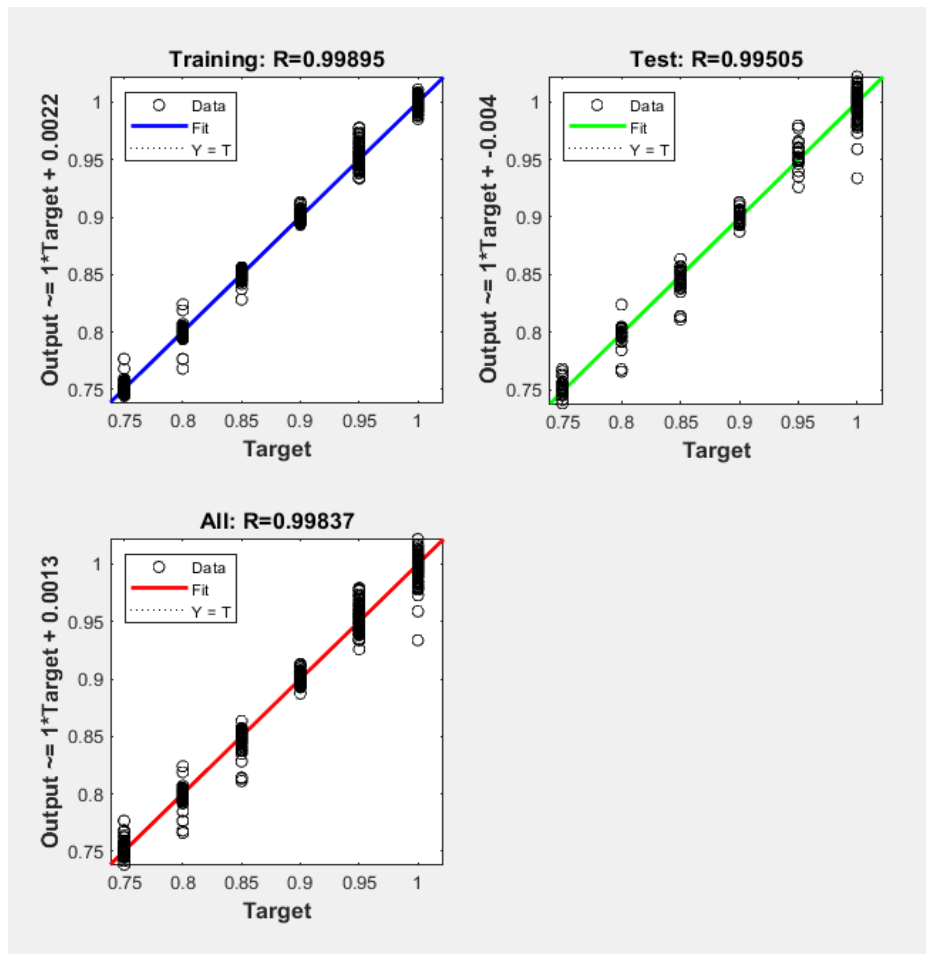


Figure 15: Training, validation and test regression plots of MMSE main network

### 6.2.1 Rib damage test

Same 08 damage cases tested on MMF network were fed into the MMSE network and the same testing procedure as discussed at MMF rib network testing was followed. Each of the test cases was first sorted to the subnetwork of relevant substructure and then the subnetwork decided the precise location and severity. Table 03 shows the damage cases tested on a trained network with the expected and received outcomes. It can be seen that the percentage errors of the test cases on the MMSE neural network are less than 0.4% and confirms the compelling performances of MMSE neural network to detect, locate and quantify damage. Further, it confirms that the MMSE network too is capable of interpolating and identifying new damage severities which are not experienced during the initial training process.

Table 03: MMSE neural network outcomes for random rib damage cases

Damage case	Absolute damage severity and location		Neural Network outcome		Percentage error in severity prediction
01	7.5%	X= 190m	<b>7.15%</b>	X= 190 m	0.38%
02	7.5%	X= 238.5m	<b>7.58%</b>	X= 238 m	-0.08%
03	12%	X= 151.5m	<b>12.14%</b>	X= 152 m	-0.16%
04	12%	X= 277.5m	<b>11.55%</b>	X= 277 m	0.5%
05	18%	X=113 m	<b>18.07%</b>	X=113 m	-0.08%
06	18%	X=203 m	<b>17.99%</b>	X=203 m	-0.009%
07	22.5%	X= 122 m	<b>22.57%</b>	X= 122 m	0.09%
08	22.5%	X= 233 m	<b>22.57%</b>	X= 233 m	0.09%

### 6.2.2 Column damage test

The same 5 column damage cases were fed into the MSE network trained for columns. The following results were obtained.

Table 04: MSE neural network outcomes for random column damage cases

Damage case	Absolute damage severity and location		Neural Network outcome		Percentage error in severity prediction
01	7.5%	Column 1 at Y=27.2m	<b>10%</b>	Column 1 at Y=27 m	-2.7%
02	7.5%	Column 2_Y= 40.2m	<b>8.2%</b>	Column 2_Y= 40 m	-0.75%
03	12%	Column 3_Y= 46.5m	<b>12.8%</b>	Column 3_Y= 46m	-0.91%
04	12%	Column 4_Y= 44.8m	<b>10.8%</b>	Column 4_Y= 44m	1.3%
05	18%	Column 5_Y= 45.2m	<b>15.8%</b>	Column 5_Y= 45m	2.68%

It is clear from the above results that the proposed neural network system along with modified DIs is capable of locating and quantifying damage in the arch rib with more than 99% accuracy and column damages with more than 97% accuracy even with noise polluted data. This paper recommends the simultaneous use of both DIs to cross-check and obtain unambiguous results.

### 6.3 Dual criteria approach and Fusion method

This study recommends two separate methods trained through two separate networks to determine damage severity and location when the damage is unknown. DIs do not always

clearly predict the damage location. False alarms can be expected due to various external factors. In such situations, the proposed dual critical approach provides the benefit of complementing and supplementing the results of each other to provide more accurate predictions of damage location.

To achieve more reliable and conclusive outcomes for unknown damages, a network fusion is proposed by combining the outcomes of the two individual neural networks (Figure 16). This is achieved by training a new neural network by combining both pre-trained neural network outcomes to obtain precise final results for unknown inputs. The inputs for the final network are the outputs from trained MMF and MMSE neural networks. Once the fusion network is trained, it is tested for unknown damage cases.

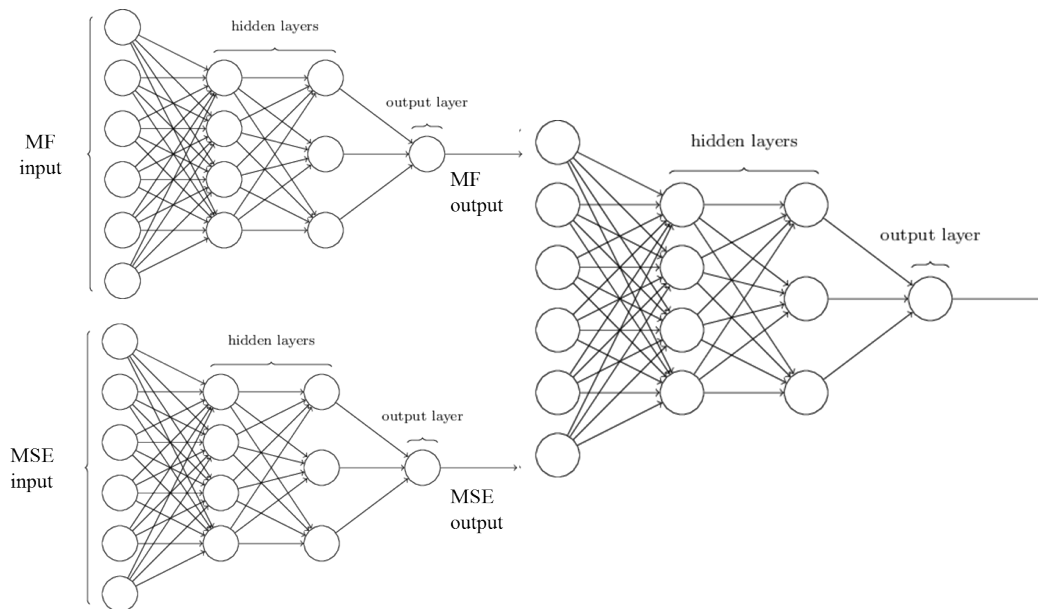


Figure 16: Combined Neural network layout

Fusion network is a regression neural network with two inputs and two outputs (Figure 17). Figure 18 presents the regression plot for fusion network created for arch rib. It is clear that the R values of all training, testing and validation networks are more than 0.99 and hence create a better convergence and trained network.

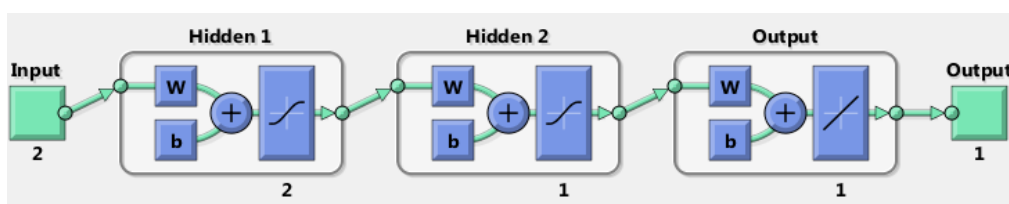




Figure 17: Fusion network configuration

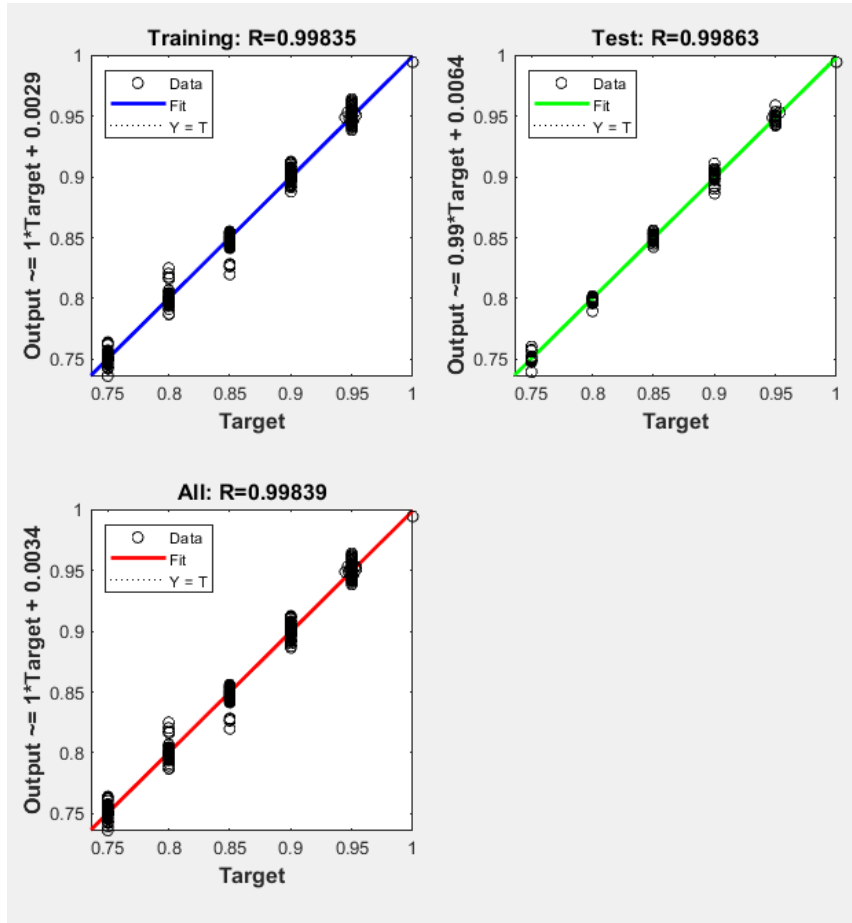


Figure 18: Training, validation and test regression plots of fusion network

Finally, the above mentioned damage test cases of arch rib and columns are tested in the fusion network and the following outputs were obtained. Table 05 and Table 06 presents the results obtained using a combined network for rib and column damage cases, respectively.

It is clear that the results are promising in determining damage location and severity. However, for some damage cases, either the MMSE or MMF neural networks can show the best prediction than the fusion network. It is natural that some networks tend to provide precise damage identification than the other. On the other hand, there can be some damage cases where one network is failed to identify correctly. In such cases, the fusion network is beneficial to identify the precise damage location and severity with close proximity to the actual damage.

Table 05: Combined neural network outcomes for random rib damage cases

Damage case	Absolute damage severity and location		Neural Network outcome		Percentage error in severity prediction
01	7.5%	X= 190m	<b>7.36%</b>	X= 190 m	0.15%
02	7.5%	X= 238.5m	<b>7.65%</b>	X= 238 m	-0.16%
03	12%	X= 151.5m	<b>12.07%</b>	X= 152 m	-0.08%
04	12%	X= 277.5m	<b>11.48%</b>	X= 277 m	0.59%
05	18%	X=113 m	<b>18.02%</b>	X=113 m	-0.02%
06	18%	X=203 m	<b>18.01%</b>	X=203 m	-0.01%
07	22.5%	X= 122 m	<b>22.55%</b>	X= 122 m	0.06%
08	22.5%	X= 233 m	<b>22.58%</b>	X= 233 m	0.11%

Table 06: Combined neural network outcomes for random column damage cases

Damage case	Absolute damage severity and location		Neural Network outcome		Percentage error in severity prediction
01	7.5%	Column 1 at Y=27.2m	<b>9.2%</b>	Column 1 at Y=27 m	-1.8%
02	7.5%	Column 2_Y= 40.2m	<b>7.6%</b>	Column 2_Y= 40 m	-0.11%
03	12%	Column 3_Y= 46.5m	<b>12.4%</b>	Column 3_Y= 46m	0.68%
04	12%	Column 4_Y= 44.8m	<b>11.2%</b>	Column 4_Y= 44m	0.9%
05	18%	Column 5_Y= 45.2m	<b>16.0%</b>	Column 5_Y= 45m	2.43%

#### 6.4 Multiple damage scenarios

It is possible to have multiple damages simultaneously during the service life of a structure. It is, therefore, necessary to check whether the neural network models developed for that particular structure is able to detect, locate and quantify multiple damage cases accurately. This study hence develops a procedure is to enhance the capabilities of a single damage neural network to detect multiple damages.

In a previous work, the modified MF and modified MSE methods have clearly shown their capacity to treat multiple damage scenarios on the rib and vertical columns of arch bridges [22]. These indices are therefore utilised to create the base parameters (which are DIs) to feed into neural networks. Firstly, few random multiple damage cases were simulated and the relevant MMF and MMSE DIs were calculated. These DIs were then tested through the

developed neural network for single damages. The results indicated that the network could not clearly distinguish the two damages simultaneously, and it picks only the higher damage case out of the two damages and expresses the output.

It is understood that the neural networks need to be modified to understand both single and multiple damage scenarios. Therefore few multiple damage cases were simulated and MMF and MMSE DI data were collected and used as ANN inputs and fed into the network trained for single damages. The amended network with new data was trained again and tested for multiple damage scenarios.

Firstly, 100 random multiple damage cases were simulated and the relevant mode shape and frequency data were obtained. These data were then used to calculate the MMF and MMSE DIs. For 5 different damage severities on 45 locations can accommodate a large number of multiple damage combinations. Therefore for the testing purposes, this study processed a limited number of random damage cases. Thus, 100 dual damages (two severities at two locations) were simulated to create data for neural network training with 4 noise levels (0%, 1%, 2% and 5%).

Once the DIs are created, those were used as the input data while the output is the damage severity and damage location. Since this part of the study used only 400 observations to train the networks, it is insufficient train the network to obtain the exact damage location (1 out of 45). Therefore, the rib was partitioned into 8 segments, instead of 45, and the output was created as to retrieve the severity and the damage segment.

The network training is performed on multi-layer feedforward network backpropagation conjugate gradient descent algorithm. The design and operation of neural networks are performed with MATLAB. Once the network is trained, it is used to detect the damage location and severity of unknown damage cases. Figure 19 presents the network configuration for MMF networks. As presented in the previous section, initially 2 networks were generated for MMF and MMSE separately. Figure 20 presents the regression plots of trained network. The results obtained from each network is fused to obtain the final damage location and severity.

Once the whole network is well trained, it is capable of testing the unknown damages and retrieve damage severity and location. Therefore, 5 multiple damage cases were randomly selected and tested through the trained neural network to obtain the damage severity and location. The final results obtained from trained neural network for damage severities and locations for 05 test damage cases are presented in Table 07 below. It was shown that the new

network is now capable of detecting and distinguishing single as well as multiple damages with their intensities (Table 07)

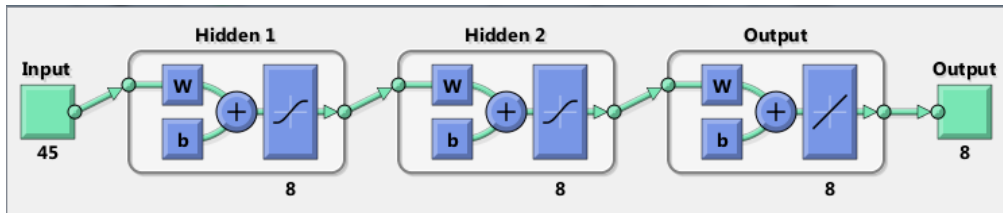


Figure 19: Regression network configuration

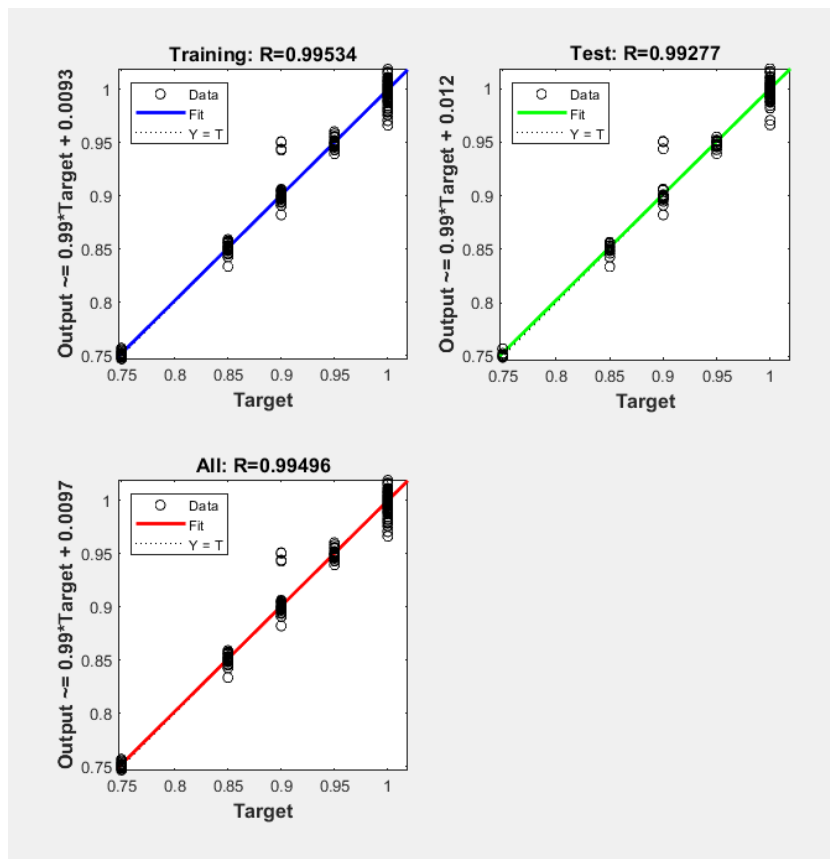


Figure20: Regression plots of training, validation and test sets for trained MMF network

Table 07: Damage severity prediction for multiple rib damages using combined network model

Damage case	Absolute damage severity and location	noise	Neural Network outcome	Percentage error
01	5% at X = 118 & 15% at X = 170	1%	4.23 % at X = 118 & 15.12% at X = 170	4.6% & 0.8%
02	20% at X=142 & 20% at X=282	2%	20.45% at X=142 & 20.7% at X=282	2.2% & 3.5%

03	7.5% at X=103 & 12% at X=248	5%	7.65% at X=103 & 11.57% at X=248	2% & 0.25%
04	12% at X =203 & 15% at X =218	5%	12.08% at X =203 & 14.8% at X =218	0.66% & 1.3%
05	22.5% at X=166 & 7.5% at X=228	2%	22.54% at X=166 & 7.87% at X=228	0.17% & 4%

## 7 Conclusion

Arch bridge structures have complex vibration characteristics which pose a challenge for using available vibration based methods to detect damage in them. Further, its complex form of damage detection, even with modified vibration based methods makes the quantification process harder and challenging. This research proposed a method designed and tested for arch bridges to detect, locate and quantify the damages in its structural components with significant accuracy. It uses the advantages of the damage index method in combination with neural network techniques to treat damages in the structural components of arch bridge. In this approach, the modified modal flexibility and modified modal strain energy based damage indices are used as base indicators to predict the damage location and to train the neural network model to locate and quantify the unknown damages.

The feasibility of the proposed procedure was illustrated via its application to assess damage in the major structural components of an arch bridge. A range of damage scenarios was considered in a (full scale) long span arch bridge involving damage in the arch rib and vertical columns. Results demonstrate the capability of the proposed method to detect, locate and quantify single and multiple damages, with reasonable accuracy, even in the presence of noise polluted data.

The dual-criteria approach was very effective in those cases where the results obtained from either DI can complement and supplement the results from the other DI and lead to a more reliable prediction of the damage location and the intensity. Reliable prediction of the damage location through the use of the proposed dual criteria approach will prevent unsafe decisions or unnecessary examinations of false alarms. Further, to achieve a more reliable and conclusive outcome for unknown damages a network fusion was proposed by combining the outcomes of two individual neural networks. The outcomes of this paper will contribute towards the safe and efficient operation of arch bridges.

## References:

- [1] P. Rizos, N. Aspragathos, A. Dimarogonas, Identification of crack location and magnitude in a cantilever beam from the vibration modes, *Journal of sound and vibration*, 138 (1990) 381-388.
- [2] J.C. Hong, Y. Kim, H. Lee, Y. Lee, Damage detection using the Lipschitz exponent estimated by the wavelet transform: applications to vibration modes of a beam, *International journal of solids and structures*, 39 (2002) 1803-1816.
- [3] H.W. Shih, D.P. Thambiratnam, T.H.T. Chan, Vibration based structural damage detection in flexural members using multi-criteria approach, *Journal of Sound and Vibration*, 323 (2009) 645-661.
- [4] P. Cornwell, S.W. Doebling, C.R. Farrar, Application of the strain energy damage detection method to plate-like structures, *Journal of sound and vibration*, 224 (1999) 359-374.
- [5] T. Contursi, A. Messina, E. Williams, A multiple-damage location assurance criterion based on natural frequency changes, *Journal of vibration and control*, 4 (1998) 619-633.
- [6] Z. Shi, S. Law, L. Zhang, Damage localization by directly using incomplete mode shapes, *Journal of Engineering Mechanics-ASCE*, 126 (2000) 656-660.
- [7] S. Law, Z. Shi, L. Zhang, Structural damage detection from incomplete and noisy modal test data, *Journal of Engineering Mechanics*, 124 (1998) 1280-1288.
- [8] S. Wang, J. Zhang, J. Liu, F. Liu, Comparative study of modal strain energy based damage localization methods for three-dimensional structure, in: The Twentieth International Offshore and Polar Engineering Conference, International Society of Offshore and Polar Engineers, 2010.
- [9] H.W. Shih, D. Thambiratnam, T.H.T. Chan, Damage detection in truss bridges using vibration based multi-criteria approach, *Structural Engineering and Mechanics*, 39 (2011) 187.
- [10] F.L. Wang, T.H.T. Chan, D.P. Thambiratnam, A.C. Tan, C.J. Cowled, Correlation-based damage detection for complicated truss bridges using multi-layer genetic algorithm, *Advances in Structural engineering*, 15 (2012) 693-706.
- [11] H. Shih, D. Thambiratnam, T.H.T. Chan, Damage detection in slab-on-girder bridges using vibration characteristics, *Structural Control and Health Monitoring*, 20 (2013) 1271-1290.
- [12] W.R. Wickramasinghe, D.P. Thambiratnam, T.H.T. Chan, T. Nguyen, Vibration characteristics and damage detection in a suspension bridge, *Journal of Sound and Vibration*, 375 (2016) 254-274.
- [13] Y. Wang, D.P. Thambiratnam, T.H.T. Chan, A. Nguyen, Damage detection in asymmetric buildings using vibration-based techniques, *Structural Control and Health Monitoring*, 25 (2018) e2148.
- [14] S.W. Doebling, Farrar, C.R., Prime, M.B. and Shevitz, D.W., , Damage identification and health monitoring of structural and mechanical systems from changes in their vibration characteristics: a literature review, Los Alamos National Lab., NM (United States). 1996.
- [15] W. Fan, P. Qiao, Vibration-based damage identification methods: a review and comparative study, *Structural Health Monitoring*, 10 (2011) 83-111.
- [16] H. Chen, C. Spyrakos, G. Venkatesh, Evaluating structural deterioration by dynamic response, *Journal of Structural Engineering*, 121 (1995) 1197-1204.
- [17] A.K. Pandey, M. Biswas, Experimental verification of flexibility difference method for locating damage in structures, *Journal of Sound and Vibration*, 184 (1995) 311-328.
- [18] H.N. Praveen Moragasipitiya, D.P. Thambiratnam, N.J. Perera, T.H.T. Chan, Development of a vibration based method to update axial shortening of vertical load bearing elements in reinforced concrete buildings, *Engineering Structures*, 46 (2013) 49-61.
- [19] T. Toksoy, A. Aktan, Bridge-condition assessment by modal flexibility, *Experimental Mechanics*, 34 (1994) 271-278.

- [20] C.R. Farrar, D.A. Jauregui, Comparative study of damage identification algorithms applied to a bridge: I. Experiment, *Smart materials and structures*, 7 (1998) 704.
- [21] N. Stubbs, J.-T. Kim, C. Farrar, Field verification of a nondestructive damage localization and severity estimation algorithm, in: Proceedings-SPIE the international society for optical engineering, SPIE INTERNATIONAL SOCIETY FOR OPTICAL, 1995, pp. 210-210.
- [22] N. Jayasundara, D. Thambiratnam, T. Chan, A. Nguyen, Vibration-based dual-criteria approach for damage detection in arch bridges, *Structural Health Monitoring*, 0 1475921718810011.
- [23] N. Caglar, Neural network based approach for determining the shear strength of circular reinforced concrete columns, *Construction and Building Materials*, 23 (2009) 3225-3232.
- [24] S.F. Jiang, C.-M. Zhang, S. Zhang, Two-stage structural damage detection using fuzzy neural networks and data fusion techniques, *Expert systems with applications*, 38 (2011) 511-519.
- [25] J.H. Park, J.-T. Kim, D.-S. Hong, D.-D. Ho, J.-H. Yi, Sequential damage detection approaches for beams using time-modal features and artificial neural networks, *Journal of Sound and Vibration*, 323 (2009) 451-474.
- [26] R.P. Bandara, T.H. Chan, D.P. Thambiratnam, Structural damage detection method using frequency response functions, *Structural Health Monitoring*, 13 (2014) 418-429.
- [27] M. Sahin, R. Shenoï, Vibration-based damage identification in beam-like composite laminates by using artificial neural networks, *Proceedings of the Institution of Mechanical Engineers, Part C: Journal of Mechanical Engineering Science*, 217 (2003) 661-676.
- [28] J. Zapico, K. Worden, F. Molina, Vibration-based damage assessment in steel frames using neural networks, *smart materials and structures*, 10 (2001) 553.
- [29] M.P. González, J.L. Zapico, Seismic damage identification in buildings using neural networks and modal data, *Computers & structures*, 86 (2008) 416-426.
- [30] J. Ko, Z. Sun, Y. Ni, Multi-stage identification scheme for detecting damage in cable-stayed Kap Shui Mun Bridge, *Engineering structures*, 24 (2002) 857-868.
- [31] J.J. Lee, C.B. Yun, Damage diagnosis of steel girder bridges using ambient vibration data, *Engineering Structures*, 28 (2006) 912-925.
- [32] H. Xu, J. Humar, Damage detection in a girder bridge by artificial neural network technique, *Computer-Aided Civil and Infrastructure Engineering*, 21 (2006) 450-464.
- [33] M. Mehrjoo, N. Khaji, H. Moharrami, A. Bahreininejad, Damage detection of truss bridge joints using Artificial Neural Networks, *Expert Systems with Applications*, 35 (2008) 1122-1131.
- [34] U. Dackermann, J. Li, B. Samali, Dynamic-based damage identification using neural network ensembles and damage index method, *Advances in Structural Engineering*, 13 (2010) 1001-1016.
- [35] N. Stubbs, G. Garcia, Application of pattern recognition to damage localization, *Computer-Aided Civil and Infrastructure Engineering*, 11 (1996) 395-409.
- [36] Z. Shi, S. Law, L. Zhang, Improved damage quantification from elemental modal strain energy change, *Journal of engineering mechanics*, 128 (2002) 521-529.
- [37] M. Sahin, R. Shenoï, Quantification and localisation of damage in beam-like structures by using artificial neural networks with experimental validation, *Engineering Structures*, 25 (2003) 1785-1802.
- [38] C. Mares, C. Surace, An application of genetic algorithms to identify damage in elastic structures, *Journal of sound and vibration*, 195 (1996) 195-215.